Published in final edited form as:
Leukemia. 2017 April ; 31(4): 957–966. doi:10.1038/leu.2016.289.

Transcriptional regulation of SPROUTY 2 by MYB influences myeloid cell proliferation and stem cell properties by enhancing responsiveness to IL-3

Mary Clarke, **Giacomo Volpe**, **Lozan Sheriff**, **David Walton**, **Carl Ward**, **Wenbin Wei**, **Stephanie Dumon**[1], **Paloma García**[1], and **Jon Frampton**[1,2]
Institute of Cancer and Genomic Sciences, College of Medical and Dental Sciences, University of Birmingham, Edgbaston, Birmingham B15 2TT, UK

Abstract

Myeloproliferative neoplasms (MPN), which overproduce blood cells in the bone marrow, have recently been linked with a genetically determined decrease in expression of the MYB transcription factor. Here, we use a mouse MYB knockdown model with an MPN-like phenotype to show how lower levels of MYB lead to stem cell characteristics in myeloid progenitors. The altered progenitor properties feature elevated cytokine responsiveness, especially to IL-3, which results from increased receptor expression and increased MAPK activity leading to enhanced phosphorylation of a key regulator of protein synthesis, ribosomal protein S6. MYB acts on MAPK signaling by directly regulating transcription of the gene encoding the negative modulator SPRY2. This mechanistic insight points to pathways that might be targeted therapeutically in MPN.

Keywords

MYB; myeloproliferative neoplasm; hematopoietic stem cells; IL-3 signaling

Introduction

Myeloproliferative neoplasms (MPN) are a heterogeneous group of hematological disorders characterized by over production of one or more myeloid lineages that can lead to the evolution of myeloid leukemia. Several genetic lesions have been described that lead to the evolution of MPN, exemplified by $JAK2^{V617F}$ and mutations in calreticulin (CALR) and the thrombopoietin receptor, MPL (1–3). Although the $JAK2^{V617F}$ mutation is associated with more than 95% of polycythemia vera (PV) and 50-60% of essential thrombocythemia (ET) and primary myelofibrosis (PMF) there are increasing reports of $JAK2^{V617F}$-negative MPN and indeed cases of MPN that are negative for mutations in JAK, MPL and CALR. Recently,

[2]Corresponding author, j.frampton@bham.ac.uk.
[1]Co-senior authors

Conflicts of Interest
The authors declare no conflicts of interest.

Europe PMC Funders Author Manuscripts

a study on MPN patients identified potential mutations that predispose to and drive the development of MPN (4). One of the polymorphisms identified was rs9376092, which is found 75 kb telomeric of the gene encoding the oncogenic transcription factor MYB. Interestingly, this risk allele is associated with reduced *MYB* RNA expression in both normal myeloid cells and $JAK2^{V617F}$ mutant BFU-E from ET patients compared to the equivalent wild type cells.

Studies on mouse models have suggested that decreased activity of MYB can lead to phenotypes that reflect at least some aspects of MPN (5, 6). We showed that reduced levels of MYB in mice homozygous for a knockdown allele ($MYB^{KD/KD}$) result in a MPN-like disorder resembling human ET, which is underpinned by a $KIT^{+}CD11b^{+}Lin^{low}$ (K11bL) cell that is stem cell like (5).

In this study we have sought to understand how a lower level of MYB in myeloid progenitors leads to a gain of stem cell characteristics and the MPN-like phenotype, and thereby shed light on the observed effect of lower MYB levels on the development of human MPN. We further characterize $MYB^{KD/KD}$ K11bL cells and show that enhanced IL-3 signaling is a key consequence of lower MYB activity. The enhanced response to IL-3 is primarily the result of an increase in MAPK signalling. We demonstrate that these changes arise at least in part from reduced activity of the signaling modulator SPROUTY2, the gene expression of which is directly regulated by MYB.

Materials and Methods

Sources of haematological tissues

Animal experiments were carried out in accordance with UK legislation. Human umbilical cord blood samples were collected with informed written consent and was approved by the NRES Committee North West – Haydock.

Flow cytometry and cell sorting

This was performed as previously described (7). All mouse antibodies are listed in Supplementary Table 1. For human CD34+ cell sorting, we used anti-CD34 PE (BD Biosciences).

Phospho-flow analysis

K11bL cells were cultured in serum-free medium for 90 min, and then stimulated with 20ng/ml IL-3 for 15 min at 37ºC. Phospho-flow was performed as previously described (8). Antibodies were PE-conjugated (Cell Signalling Technology). For inhibition experiments, cells were pre-treated with either 1μM Rapamycin or 10μM U0126 (Sigma) in serum-free media at 37°C for 1 hour.

Engraftment potential of stem cells

Cell transplantation experiments were carried as previously described (5) with 10 000 K11bL (CD45.2/CD45.2) cells injected together with $3x10^5$ reference (CD45.1/CD45.2) bone marrow cells.

Homing assays

Sorted K11bL cells were labeled with 0.3 mg/ml Xenolight DiR (Caliper Life Sciences) for 30 min at 37°C. Cells were washed and re-suspended in 150μl of PBS, and injected via the tail vein into lethally irradiate hosts (B6:SJL). Details of IVIS imaging conditions can be found in Supplementary Information.

Transfection and cell culture

Human $CD34^+$ were sorted and transfected using the 4D-Nucleofector system (Lonza) with FAM-labeled siRNAs (Supplementary Table 2). Following transfection, $CD34^+$ cells were cultured for 24 hours in RPMI supplemented with 10% FBS, 50ng/ml SCF, 10ng/ml IL3 and 20ng/ml IL6. After 24 hours cells were plated in complete methylcellulose (Methocult GF H84435). Colony morphology and number were assessed between 7-14 days.

Transduction of bone marrow cells

Lentiviruses (Origene) expressing shRNA *SPRY2* (TG515588) or *Il3ra* (TG516353) or *SPRY2* ORF together with GFP, were generated as described (9). Bone marrow or K11bL cells were cultured in the presence of 3μg/ml Polybrene (Sigma) with lentivirus at an MOI of 10. Cells were cultured for 4 hours, washed and either injected into lethally irradiated mice or further cultured for 20 hours. Infection efficiency was assessed based on GFP expression.

Gene expression analysis

Affymetrix Mouse Gene 1.0 ST array analysis was performed on K11bL cells. The GEO accession number for the data deposited is GSE74140. Further detail can be found in Supplementary Information. Quantitative PCR was performed as previously described (5). TaqMan PCR primers (Applied Biosystems) and primer sequences are listed in Supplementary Table 3.

X-ChIP analysis

X-ChIP assays were performed as previously described (10) using antibodies from Santa Cruz Biotechnology and anti-MYB antibody from Merck Millipore. Primers for detection of MYB binding to the *SPRY2* and *DUSP6* genes are listed in Supplementary Table 4.

Statistical analysis

Significance of data sets was assessed using two-tailed unpaired Student's t-test with significance set at $p<0.05$.

Results

$MYB^{KD/KD}$ K11bL cells exhibit myeloid bias and have stem cell characteristics

When K11bL cells, which are more abundant in $MYB^{KD/KD}$ mice compared to $MYB^{WT/WT}$ controls (Figure 1A), were transplanted into lethally irradiated mice they engrafted significantly, irrespective of whether they were $MYB^{WT/WT}$ or $MYB^{KD/KD}$ (Supplementary Figure 1A). However, engrafted $MYB^{KD/KD}$ K11bL cells gave rise predominantly in the

peripheral blood to CD11b^{+} myelomonocytic cells whereas *MYB*$^{WT/WT}$ K11bL cells largely differentiated into B220^{+} B-lymphoid cells (Figure 1B), and all bone marrow K11bL cells derived from *MYB*$^{KD/KD}$ donor cells were positive for CD41 (Supplementary Figure 1B). Importantly, when bone marrow isolated from the primary recipients was transplanted into secondary hosts, *MYB*$^{WT/WT}$ K11bL cells failed to support serial engraftment, whereas *MYB*$^{KD/KD}$ cells were able to perpetuate the myeloproliferative phenotype (Supplementary Figure 1C).

We confirmed the *MYB*$^{KD/KD}$ lineage bias of K11bL cells by in vitro colony assay. *MYB*$^{KD/KD}$ cells predominantly formed CFU-M and CFU-M/Mk colonies, failing to produce colonies of granulocytic or erythroid morphology, whereas *MYB*$^{WT/WT}$ K11bL cells were able to undergo a full program of myeloid differentiation (Supplementary Figure 1D). Microarray analysis of K11bL cells confirmed the shift from a lymphoid to a myeloid bias, Gene Ontogeny (GO) analysis showing that compared to *MYB*$^{WT/WT}$ K11bL cells, *MYB*$^{KD/KD}$ cells exhibit higher expression of genes associated with myeloid differentiation, and reduced levels of lymphoid-associated genes (Supplementary Table 5).

We sought to identify the differences in surface marker and gene expression that might explain the stem cell-like transplantation behaviour of *MYB*$^{KD/KD}$ K11bL cells (Figure 1Ci and Supplementary Figure 1E). *MYB*$^{KD/KD}$ K11bL cells have higher levels of expression of the integrins CD51 (α_V), CD41 (αIIb) and CD61 (β3) and the adhesion molecule CD62 (P-selectin). Since *MYB*$^{KD/KD}$ K11bL cells have gained stem cell properties, we analysed the microarray for expression of homing and bone marrow retention molecules together with flow cytometric analysis of some of the key proteins. Analysis of RNA expression data for the GO group “cell chemotaxis” (GO:0060326) revealed an increase in expression of genes associated with homing and invasion of extramedullary sites of hematopoiesis (eg *Ccr1*) and lower levels of genes regulating bone marrow retention (eg *Vcam1*) (Supplementary Table 6). Flow cytometric analysis confirmed the reduction of VCAM1 on the surface of *MYB*$^{KD/KD}$ K11bL cells (Figure 1Cii and Supplementary Figure 1E). Consistent with their stem cell characteristics, *MYB*$^{KD/KD}$ K11bL cells have higher levels of SCA1 and CD34, and exhibit a small but significantly higher level of the SLAM marker CD150 ($p \leq 0.01$) (Figure 1Ciii and Supplementary Figure 1E).

MYB$^{KD/KD}$ K11bL cells have an enhanced response to IL-3

Interestingly, analysis of genes in the GO group “cytokine-mediated signaling pathway” (GO:0019221) revealed that a number of cytokine receptor genes are more highly expressed in *MYB*$^{KD/KD}$ K11bL cells compared to the *MYB*$^{WT/WT}$ equivalent. Amongst these genes we identified *CSF2RB* (*IL3RBC*) as being more highly expressed in *MYB*$^{KD/KD}$ K11bL cells (2.25-fold $p=7\times10^{-5}$ Supplementary Table 7). This difference, together with that of the other IL-3 receptor component *IL3RA,* was confirmed by quantitative PCR (Figure 2A). Correspondingly, immunofluorescence analysis showed that the expression of IL3RA (CD123) and CSF2RB (CD131) are greater on *MYB*$^{KD/KD}$ K11bL cells than the *MYB*$^{WT/WT}$ equivalents (Supplementary Figure 2A).

It is well documented that malignant cells can exhibit a heightened response to growth factors, augmenting their proliferation and survival. Our observations on altered IL-3

receptor expression on $MYB^{KD/KD}$ K11bL cells combined with the fate of the cells following transplantation led us to ask if altered responses to IL-3 could be dictating stem cell characteristics. When we plated cells in semi-solid media containing a range of concentrations of IL-3, this revealed that $MYB^{KD/KD}$ K11bL cells have a heightened response to the cytokine as manifested by higher colony numbers. This enhancement was significant at all concentrations tested down to 0.02ng/ml ($p \leq 0.05$) (Figure 2B). Analysis of colony morphology showed that $MYB^{WT/WT}$ K11bL cells yielded colonies containing granulocytes (CFU-G), macrophage (CFU-M), and a mix of both of these cell types (CFU-GM). In contrast, $MYB^{KD/KD}$ cells formed mainly CFU-M, which were highly proliferative and gave rise to disperse colonies as well as a few colonies containing both macrophages and megakaryocytes (Figure 2C).

IL-3 signaling is critical for $MYB^{KD/KD}$ K11bL cell function

To determine how dependent $MYB^{WT/WT}$ and $MYB^{KD/KD}$ K11bL cells are on signaling through the IL-3 receptor, even in the presence of other growth factors, we used a neutralizing antibody against the IL-3 receptor subunit IL3RB to inhibit the response to IL-3. We observed a marked reduction in colony number from 19±1 to 8±0 ($p=0.004$) for $MYB^{KD/KD}$ K11bL cells, but saw no effect on $MYB^{WT/WT}$ cells (Figure 3A), suggesting that $MYB^{KD/KD}$ K11bL cells are critically dependent on signaling through the IL-3 receptor.

Since IL3RB is common to signaling through both the IL-3 and GM-CSF receptors, we wanted directly to assess the effect of knocking down the other IL-3-specific subunit, IL3RA. $MYB^{KD/KD}$ K11bL cells were transduced with lentivirus expressing *IL3RA* shRNA and were then transplanted into lethally irradiated mice. Co-expression of GFP from the shRNA vector indicated that we achieved a transduction rate of ~70% (Figure 3Bi). Engraftment was apparent after one month, however the proportion of donor cells in the peripheral blood was markedly reduced when IL3RA was knocked down. By 3 months this difference was more evident (Figure 3Bii). Interestingly, $MYB^{KD/KD}$ donor cells expressing shRNA *IL3RA* had a significantly reduced differentiation towards monocytes ($Gr1^{-}CD11b^{+}$) compared to control cells (69±3% compared to 57±2%, $p \leq 0.01$) and a corresponding increase in differentiation towards granulocytes ($Gr1^{+}CD11b^{+}$) (Supplementary Figure 2B). Similar to previous observations, the ratio of shRNA control transduced donor $MYB^{KD/KD}$ cells rapidly increased between 1 and 7 months following transplantation, whereas the cells expressing shRNA *IL3RA* were maintained at their low engraftment ratio, indicating a necessity for the expression of IL3RA for engraftment of $MYB^{KD/KD}$ K11bL cells (Supplementary Figure 2C).

The influence of enhanced IL-3 signaling on engraftment was further examined with respect to short term migration and homing following transplantation. Following injection of fluorescently labeled K11bL cells it was evident after one hour that the $MYB^{KD/KD}$ cells have distinct homing behavior compared to $MYB^{WT/WT}$ K11bL cells, with the predominant signal emanating from the spleen. Using the IL3RB blocking antibody we then showed that active signaling through IL3RB is required for the ability of $MYB^{KD/KD}$ K11bL cells to home towards the spleen as evidenced by a loss of fluorescence signal (9±1 to 0.44±0.2 photon/s $p=0.007$) when IL3RB was blocked (Figure 3C and Supplementary Figure 2D).

Signaling downstream of the IL-3 receptor is enhanced in *MYB*$^{KD/KD}$ K11bL cells

We used phospho-flow cytometry to determine if the enhanced response of *MYB*$^{KD/KD}$ K11bL cells is reflected in the phosphorylation status of molecules that could influence the interpretation of IL-3-mediated signaling. The only significant difference in steady-state phosphorylation was observed in rpS6$^{Ser235/236}$ and STAT5^{Tyr694}, the former exhibiting a median fluorescence intensity (MFI) of 18.9±1.1 in *MYB*$^{WT/WT}$ K11bL cells versus 52.5±2.4 (p=0.003) in *MYB*$^{KD/KD}$ cells and the latter being 26.4±1.5 in *MYB*$^{WT/WT}$ compared to 47.9±0.3 (p=0.0026) in *MYB*$^{KD/KD}$ cells (Supplementary Figure 3A).

In order to assess the effect of IL-3 stimulation on the dynamics of phosphorylation, K11bL cells were starved of serum prior to stimulation with IL-3 and subsequent analysis 15 min later. We observed differences in both the extent of the response and the relative degree of phosphorylation of rpS6$^{Ser235/236}$ and rpS6$^{Ser240/244}$. Hence, stimulation of K11bL cells with IL-3 led to an increase in rpS6$^{Ser235/236}$ phosphorylation, reflected in a MFI shift of 105±36 to 232±32 (p=0.009) for *MYB*$^{WT/WT}$ and 91±29 to 480±82 (p=0.0002) for *MYB*$^{KD/KD}$ (Figure 4Ai and Supplementary Figure 3B). This also revealed that *MYB*$^{KD/KD}$ K11bL cells showed a significantly greater increase in the proportion of cells phosphorylated at this site and reached an overall higher level of phosphorylation, the MFI being twice as great as that seen in *MYB*$^{WT/WT}$ K11bL cells (p=0.0063; Supplementary Figure 3B). We therefore also checked for changes in phosphorylation at the rpS6$^{Ser240/244}$ site. Following IL-3 stimulation, no significant increase in phosphorylation was seen in *MYB*$^{WT/WT}$ K11bL cells, whereas *MYB*$^{KD/KD}$ K11bL cells demonstrated a small increase, seen as a shift in MFI of 13.3±3 to 22.9±4 (p=0.02) (Figure 4Ai and Supplementary Figure 3C).

Phosphorylation of rpS6$^{Ser235/236}$ can occur through activation of the PI3k/AKT/mTOR or RAS/MAPK pathways, whereas only the former leads to the modification of rpS6$^{Ser240/244}$ (11). We examined the phosphorylation status of AKT (Thr308 and Ser473) and p44/42 MAPK (ERK1/2) to investigate the relative use of the two pathways. At 15 min post IL-3 stimulation we failed to detect any phosphorylation of AKT or p44/42 MAPK (data not shown). However, reasoning that the response to IL-3 might be very rapid, we also looked at phosphorylation at 5 min following IL-3 addition. A significant increase in phosphorylation of AKT^{Thr308} was seen as a shift in MFI from 6.7±1.5 to 13.8±4.5 (p=0.047) (Figure 4Aii and Supplementary Figure 3D). We also observed an increase in the percentage of cells positive for p44/42 MAPK phosphorylation from 4±3% to 23±5% (p=0.04) in *MYB*$^{KD/KD}$ K11bL cells but not in the *MYB*$^{WT/WT}$ equivalent (Figure Aii and Supplementary Figure 3E).

To confirm the dependence of rpS6 phosphorylation on the PI3k/AKT/mTOR and RAS/MAPK pathways and better to define how the specificity and balance of activity differs in *MYB*$^{KD/KD}$ K11bL cells compared to *MYB*$^{WT/WT}$ cells, we performed IL-3 stimulations following pre-treatment of the K11bL cells with inhibitors of mTOR (Rapamycin) or MEK (U0126). Treatment of *MYB*$^{WT/WT}$ cells with Rapamycin but not U0126 resulted in a loss of phosphorylation of rpS6$^{Ser235/236}$ from 21.8±3.2% to 12.5±2.7% (p=0.02, Supplementary Figure 3F).Similar analysis of rpS6 in *MYB*$^{KD/KD}$ K11bL cells showed that phosphorylation at Ser235/236 was inhibited by U0126 (45.5±7.1% to 13.7±3.5%; p=9.5x10^{-05}) but not by

Rapamycin, whereas the Ser240/244 site modification was susceptible to inhibition of mTOR but not MEK (Figure 4B and Supplementary Figure 3F). This implies that one aspect of the distinctive cytokine responsiveness seen in *MYB*$^{KD/KD}$ K11bL cells relates to a shift in the relative usage of the signaling pathways downstream of the IL-3 receptor.

The baseline phosphorylation of STAT5^{Tyr694} was lower in *MYB*$^{KD/KD}$ K11bL cells but upon stimulation with IL-3 increased to a level similar to that seen in *MYB*$^{WT/WT}$ cells following their treatment with cytokine (Figure 4Ci). Consistent with the phosphorylation of STAT5 being elicited through a JAK protein, we observed no effect on the level of phosphorylation in the presence of the mTOR or MEK inhibitors (Figure 4Cii).

The expression of signaling-associated genes defines the *MYB*$^{KD/KD}$ K11bL phenotype

Based on the phosphorylation results, we further analysed the array data to look at GO groups associated with signaling. Analysis of deregulated genes involved in intracellular signal transduction (GO:1902532) (Supplementary Table 8) and in particular proteins involved in the ERK signalling cascade (GO:0070372) (Supplementary Table 9) highlighted the altered expression of several genes. In particular, we noted that *MYB*$^{KD/KD}$ K11bL cells exhibit lower expression of the genes encoding the inhibitor SPROUTY2 (*SPRY2*), the dual specificity phosphatase 6 (*DUSP6*), and the RAS protein activator (*RASA2*), and higher expression of dual specificity phosphatase 3 (*DUSP3*), and suppressor of cytokine signalling 3 (*SOCS3*).

In order to confirm which of these differences might reflect direct regulation by MYB we used our conditional *MYB* knockout (12). K11bL cells were isolated from control mice (*MYB*$^{+/+}$*:Cre*) and *MYB* knockout (*MYB*$^{F/F}$*:Cre*) mice 24 hours after induction of deletion, and the levels of RNA for *MYB* and the selected genes were measured by quantitative RT-PCR. This confirmed that *SPRY2* and *DUSP6* RNA levels were depleted, whilst the levels of *IL3RA, CSF2RB, CSFR2RB2, CSFR1, SOCS3, DUSP3, MECOM,* and *CCND1* were higher, suggesting that the expression of these genes could be directly inhibited by MYB (Figure 5A).

MYB directly regulates expression of the *SPRY2* and *DUSP6* genes

We next used X-ChIP to determine if positive regulation of the *SPRY2* and *DUSP6* genes by MYB correlates with binding of the protein to gene regulatory regions. We prepared chromatin from the murine HSC line HPC-7 (13), and used an antibody against MYB for immunoprecipitation of *SPRY2* and *DUSP6* gene fragments corresponding to *in vivo* binding sites for the factor. Primers for quantitative PCR were designed around highly conserved regions that contained potential MYB binding sequences. In this way, we demonstrated MYB binding to the *SPRY2* promoter (-0.55kb from ATG, Figure 5B) and the *DUSP6* promoter (-2.7kb from ATG, Figure 5C), whereas there was no significant enrichment of either the *SPRY2* enhancer (-26kb from ATG) or the *DUSP6* distal promoter (-2.7kb from ATG) (Supplementary Figure 4).

Reduced MYB expression in human progenitors mirrors the changes seen in *MYB*$^{KD/KD}$ K11bL cells

To examine if our observations in the mouse system are paralleled in human cells we transfected CD34+ cord blood cells with *MYB* siRNA. This achieved a 50% reduction in *MYB* gene expression at 24 hours, and upon plating cells in methylcellulose containing myeloid growth factors we observed that knockdown of MYB leads to an increase in CFU-M and CFU-Mk and a reduction in CFU-G, CFU-GEMM and BFU-E, in line with the broad phenotypic changes seen in *MYB*$^{KD/KD}$ K11bL cells (Figure 6A). We also showed that the knockdown of MYB in the human cells led to a significant decrease in the expression of *SPRY2* and increased expression of *IL3RA* and *CSF1R,* exactly as we saw in murine *MYB*$^{KD/KD}$ K11bL cells, however, unlike in mouse K11bL cells, the expression of *DUSP6* was significantly increased (Figure 6B).

Manipulation of *SPRY2* expression in *MYB*$^{WT/WT}$ cells partially recapitulates the *MYB*$^{KD/KD}$ stem cell phenotype

Based on the apparent importance of enhanced IL-3-dependent RAS/MAPK signaling in *MYB*$^{KD/KD}$ K11bL cells and the conserved MYB-dependent expression of *SPRY2* in both mouse and human progenitor cells, we reasoned that SPRY2 is pivotal to the way in which IL-3 can influence stem cell characteristics of myeloid progenitors. In order to assess the degree to which SPRY2 is responsible for the gain of stem cell function, we transduced *MYB*$^{WT/WT}$ K11bL cells with a lentiviral vector expressing shRNA directed against *SPRY2* and assayed their ability to form hematopoietic colonies *in vitro*. *MYB*$^{WT/WT}$ K11bL cells transduced with control virus demonstrated normal colony formation in complete methylcellulose. In contrast, *MYB*$^{WT/WT}$ cells transduced with lentivirus expressing *SPRY2* shRNA (which exhibited >95% knockdown - Supplementary Figure 5A) demonstrated reduced CFU-G colonies and increased CFU-M colonies, similar to the situation seen for *MYB*$^{KD/KD}$ K11bL cells (Figure 7A). Secondary plating of *MYB*$^{WT/WT}$ K11bL cells experiencing *SPRY2* knockdown resulted in colonies that covered the plate, whereas control cells formed very small, sparsely distributed colonies (Supplementary Figure 5B). These *SPRY2* knockdown *MYB*$^{WT/WT}$ K11bL secondary colonies showed increased levels of KIT and CD34 compared to the control cells (Supplementary Figure 5C).

Transplantation assays of *MYB*$^{WT/WT}$ K11bL cells transduced with control or *SPRY2* shRNA revealed a higher donor to reference ratio when levels of *SPRY2* were reduced (Figure 7B). This enhanced engraftment was further amplified by 3 months but the contribution to peripheral myeloid cells (CD11b+) was not altered (Supplementary Figure 5D). Secondary transplantation revealed the acquisition of long-term repopulating ability by the *SPRY2* knockdown K11bL cells (Supplementary Figure 5E). We then asked if over expression of *SPRY2* in *MYB*$^{KD/KD}$ K11bL cells could reverse their proliferation and differentiation characteristics. Colony forming assays of *MYB*$^{KD/KD}$ K11bL cells transduced with a lentivirus expressing *SPRY2* resulted in a significant reduction in colony number in complete methylcellulose (Figure 7C). Additionally the *SPRY2*-overexpressing *MYB*$^{KD/KD}$ K11bL cells gave rise to a lower proportion of megakaryocyte colonies and increased granulocytic colonies compared to K11bL cells infected with control virus (Figure 7C).

Discussion

MYB was originally shown to be a critical regulator of hematopoiesis since complete ablation abolished definitive hematopoiesis (14). The role that MYB plays in adult hematopoiesis has been studied using mouse models with reduced activity of the protein (5, 6, 12, 15), revealing a role for MYB in immature proliferating hematopoietic cells. Here we have sought to link recent observations on the genetic predisposition to MPN caused by lower levels of expression of MYB (4) with the phenotype seen in our mouse model for decreased MYB activity. We show that lower MYB levels in myeloid progenitors results in; (i) altered short-term homing towards the spleen, (ii) differentiation towards myelomonocytic cells, and (iii) a stem cell phenotype, including self-renewal potential that is not seen in the normal equivalents and giving a phenotype more similar to those described in some chronic myeloid leukemia (CML) and acute promyelocytic leukemia (APL) stem cells (16, 17).

Key to the $MYB^{KD/KD}$ phenotype is altered IL-3 signaling, particularly along the RAS/MAPK pathway. Our results suggest that enhanced IL-3 signaling is responsible for aspects of the aberrant stem cell phenotype, including homing to the spleen, engraftment potential, and lineage bias. Such acquired properties likely have relevance to the leukemia stem cell-specific role of IL-3 receptor in acute myeloid leukemia (AML), which has been shown to be an effective target for an anti-IL3RA (CD123) antibody (18).

We are presently investigating the mechanisms by which increased IL-3-dependent signaling leads to the $MYB^{KD/KD}$ phenotype. The RAS/MAPK pathway appears to be central and, although the nature of the critical targets remains unclear, we found evidence for the activation of ribosomal protein S6, which itself plays an essential role in protein translation of several pro-survival protein genes such as MYC, BCL-XL, and SURVIVIN, and might therefore contribute to the gain of stem cell properties. Interestingly, there are descriptions of the importance of ERK/MAPK in self-renewal of both embryonic and adult stem cells (19, 20). The RAS/MAPK pathway is frequently activated in hematological malignancy and has been implicated in the sensitivity and resistance of cells to therapy (21), including in other MPN models such as the KRAS mutant mouse (22).

We explored the mechanisms by which reduced MYB activity leads to enhanced IL-3 signaling, and found that these involved multiple direct and indirect targets, and including both positively and negatively regulated genes. Aside from what appears to be coordinated positive regulation of several cytokine receptor genes, MYB also normally seems to provide a coordinated controlling influence on RAS/MAPK signaling by promoting the expression of negative pathway regulators, including SPRY2 and DUSP6. SPRY2, which prevents the interaction between RAS and GRB2-SOS (23) following their recruitment by SHC when it associates with the IL-3 receptor, seems to be relevant in both the mouse and human systems we examined. The lower expression of SPRY2 would be expected to release the inhibition of RAS, leading to an increased sensitivity to IL-3. Interestingly, knockdown of *SPRY2* in wild type progenitor cells both shifted their phenotype and enhanced engraftment potential, partially reflecting the overall phenotype of the $MYB^{KD/KD}$ cells.

We postulate a working model for the signaling pathways utilized in K11bL cells in both $MYB^{WT/WT}$ and $MYB^{KD/KD}$ mice (Figure 8), and clearly our study has opened up a whole new chapter in the understanding of the pivotal role of MYB in both normal and malignant hematopoiesis. Although numerous additional mechanisms undoubtedly combine to give rise to the complete $MYB^{KD/KD}$ MPN-like phenotype, our findings suggest that IL-3-dependent signaling plays a major role, affecting the regulation of genes responsible for migration, proliferation, and differentiation. For those hematological disorders where MYB activity is affected, including MPN, the knowledge that signaling downstream of IL-3 receptor is affected as a direct result of altered MYB levels could open up the possibility for a more direct approach to treatment.

Supplementary Methods

Bone marrow cell isolation and culture

All mice were maintained on a C57/BL6 background and sacrificed at 4 weeks of age as a source of bone marrow. Conditional deletion of *MYB* was induced by intraperitoneal injection of 250μg poly(inosinic-cytidylic) acid (pIpC, Sigma) and 24 hours later were sacrificed for bone marrow analysis. Peripheral blood was collected from the tail vein into acid citrate dextrose (ACD) solution. Sorted mouse K11bL cells were plated in complete methylcellulose medium (Methocult M3434, Stem Cell Technologies) containing TPO (25ng/ml). Methocult lacking growth factors (M3234) was used to assess the response to specific cytokines.

Homing assays

For live animal imaging, mice were shaved and imaged using an IVIS spectrum under 2.5% iso-fluorane (Caliper Life Sciences). Mice were imaged ventrally at 1 and 24 hours. Images were acquired by trans-illumination at 745nm excitation and 800nm emission with exposure times ranging from 1.4 seconds to 60 seconds, medium binning and f-stop 2. IVIS data was analysed using Living Image 4.0 software (Caliper Life Sciences).

Gene expression analysis

Scanned images of microarrays were analyzed using the Affymetrix GeneChip Command Console. Probe level quantile normalization (24) and robust multi-array analysis (25) on the raw CEL files were performed using Affymetrix Expression Console. Differentially expressed genes were identified using limma with absolute fold change >1.5 and $p<0.01$ (26). Gene ontogeny was analysed using Gene Ontology Enrichment Analysis Software Toolkit (GOEAST).

Supplementary Material

Refer to Web version on PubMed Central for supplementary material.

Acknowledgments

This work was supported entirely by Bloodwise.

References

1. Campbell PJ, Green AR. The myeloproliferative disorders. N Engl J Med. 2006; 355(23):2452–66. [PubMed: 17151367]
2. Klampfl T, Gisslinger H, Harutyunyan AS, Nivarthi H, Rumi E, Milosevic JD, et al. Somatic mutations of calreticulin in myeloproliferative neoplasms. N Engl J Med. 2013; 369(25):2379–90. [PubMed: 24325356]
3. Pardanani AD, Levine RL, Lasho T, Pikman Y, Mesa RA, Wadleigh M, et al. MPL515 mutations in myeloproliferative and other myeloid disorders: a study of 1182 patients. Blood. 2006; 108(10): 3472–6. [PubMed: 16868251]
4. Tapper W, Jones AV, Kralovics R, Harutyunyan AS, Zoi K, Leung W, et al. Genetic variation at MECOM, TERT, JAK2 and HBS1L-MYB predisposes to myeloproliferative neoplasms. Nat Commun. 2015; 6:6691. [PubMed: 25849990]
5. Garcia P, Clarke M, Vegiopoulos A, Berlanga O, Camelo A, Lorvellec M, et al. Reduced c-Myb activity compromises HSCs and leads to a myeloproliferation with a novel stem cell basis. EMBO J. 2009; 28(10):1492–504. [PubMed: 19360001]
6. Lieu YK, Reddy EP. Conditional c-myb knockout in adult hematopoietic stem cells leads to loss of self-renewal due to impaired proliferation and accelerated differentiation. Proc Natl Acad Sci U S A. 2009; 106(51):21689–94. [PubMed: 19955420]
7. Clarke M, Dumon S, Ward C, Jager R, Freeman S, Dawood B, et al. MYBL2 haploinsufficiency increases susceptibility to age-related haematopoietic neoplasia. Leukemia. 2013; 27(3):661–70. [PubMed: 22910183]
8. Krutzik PO, Nolan GP. Intracellular phospho-protein staining techniques for flow cytometry: monitoring single cell signaling events. Cytometry A. 2003; 55(2):61–70. [PubMed: 14505311]
9. Sommer CA, Stadtfeld M, Murphy GJ, Hochedlinger K, Kotton DN, Mostoslavsky G. Induced pluripotent stem cell generation using a single lentiviral stem cell cassette. Stem Cells. 2009; 27(3): 543–9. [PubMed: 19096035]
10. Dumon S, Walton DS, Volpe G, Wilson N, Dasse E, Del Pozzo W, et al. Itga2b regulation at the onset of definitive hematopoiesis and commitment to differentiation. PLoS One. 2012; 7(8):e43300. [PubMed: 22952660]
11. Roux PP, Shahbazian D, Vu H, Holz MK, Cohen MS, Taunton J, et al. RAS/ERK signaling promotes site-specific ribosomal protein S6 phosphorylation via RSK and stimulates cap-dependent translation. J Biol Chem. 2007; 282(19):14056–64. [PubMed: 17360704]
12. Emambokus N, Vegiopoulos A, Harman B, Jenkinson E, Anderson G, Frampton J. Progression through key stages of haemopoiesis is dependent on distinct threshold levels of c-Myb. EMBO J. 2003; 22(17):4478–88. [PubMed: 12941699]
13. Pinto do OP, Kolterud A, Carlsson L. Expression of the LIM-homeobox gene LH2 generates immortalized steel factor-dependent multipotent hematopoietic precursors. EMBO J. 1998; 17(19): 5744–56. [PubMed: 9755174]
14. Mucenski ML, McLain K, Kier AB, Swerdlow SH, Schreiner CM, Miller TA, et al. A functional c-myb gene is required for normal murine fetal hepatic hematopoiesis. Cell. 1991; 65(4):677–89. [PubMed: 1709592]
15. Sandberg ML, Sutton SE, Pletcher MT, Wiltshire T, Tarantino LM, Hogenesch JB, et al. c-Myb and p300 regulate hematopoietic stem cell proliferation and differentiation. Dev Cell. 2005; 8(2):153–66. [PubMed: 15691758]
16. Guibal FC, Alberich-Jorda M, Hirai H, Ebralidze A, Levantini E, Di Ruscio A, et al. Identification of a myeloid committed progenitor as the cancer-initiating cell in acute promyelocytic leukemia. Blood. 2009; 114(27):5415–25. [PubMed: 19797526]
17. Bruns I, Czibere A, Fischer JC, Roels F, Cadeddu RP, Buest S, et al. The hematopoietic stem cell in chronic phase CML is characterized by a transcriptional profile resembling normal myeloid progenitor cells and reflecting loss of quiescence. Leukemia. 2009; 23(5):892–9. [PubMed: 19158832]

18. Jin L, Lee EM, Ramshaw HS, Busfield SJ, Peoppl AG, Wilkinson L, et al. Monoclonal antibody-mediated targeting of CD123, IL-3 receptor alpha chain, eliminates human acute myeloid leukemic stem cells. Cell Stem Cell. 2009; 5(1):31–42. [PubMed: 19570512]
19. Chen H, Guo R, Zhang Q, Guo H, Yang M, Wu Z, et al. Erk signaling is indispensable for genomic stability and self-renewal of mouse embryonic stem cells. Proc Natl Acad Sci U S A. 2015; 112(44):E5936–43. [PubMed: 26483458]
20. Geest CR, Coffer PJ. MAPK signaling pathways in the regulation of hematopoiesis. J Leukoc Biol. 2009; 86(2):237–50. [PubMed: 19498045]
21. Malumbres M, Barbacid M. RAS oncogenes: the first 30 years. Nat Rev Cancer. 2003; 3(6):459–65. [PubMed: 12778136]
22. Lyubynska N, Gorman MF, Lauchle JO, Hong WX, Akutagawa JK, Shannon K, et al. A MEK inhibitor abrogates myeloproliferative disease in Kras mutant mice. Sci Transl Med. 2011; 3(76): 76ra27.
23. Yusoff P, Lao DH, Ong SH, Wong ES, Lim J, Lo TL, et al. Sprouty2 inhibits the Ras/MAP kinase pathway by inhibiting the activation of Raf. J Biol Chem. 2002; 277(5):3195–201. [PubMed: 11698404]
24. Bolstad BM, Irizarry RA, Astrand M, Speed TP. A comparison of normalization methods for high density oligonucleotide array data based on variance and bias. Bioinformatics. 2003; 19(2):185–93. [PubMed: 12538238]
25. Irizarry RA, Bolstad BM, Collin F, Cope LM, Hobbs B, Speed TP. Summaries of Affymetrix GeneChip probe level data. Nucleic Acids Res. 2003; 31(4):e15. [PubMed: 12582260]
26. Smyth GK. Linear models and empirical bayes methods for assessing differential expression in microarray experiments. Stat Appl Genet Mol Biol. 2004; 3 Article3.

Europe PMC Funders Author Manuscripts

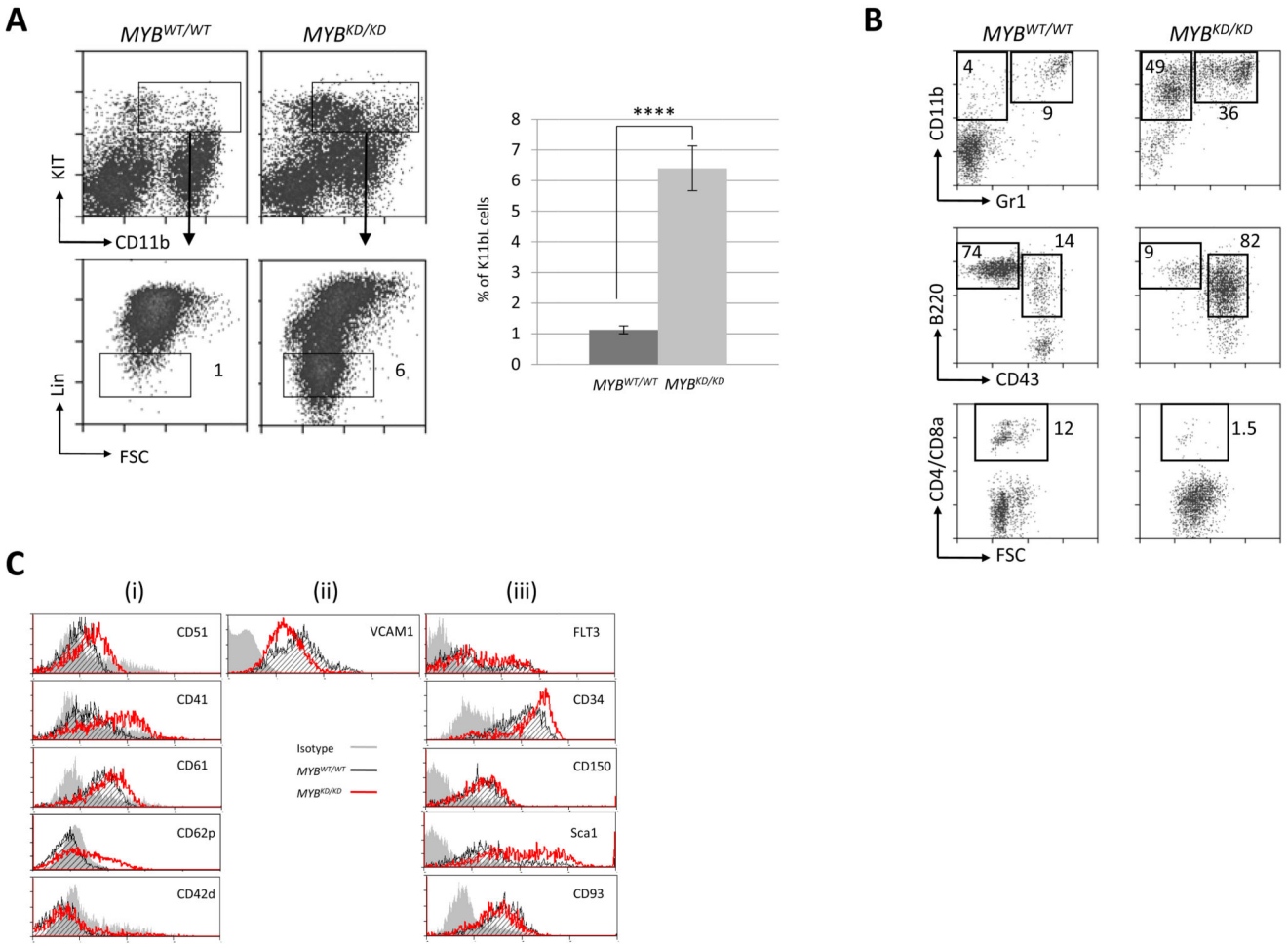

Figure 1.

A) Whole bone marrow cells were gated for expression of KIT and CD11b and then analysed for expression of lineage markers ****p≤0.0001. B) Primary donor-derived cells in the peripheral blood analyzed for expression of myeloid, B-cell, and T-cell markers at 3 months post-transplantation. Numbers represent average percentage of total cells. C) Representative (N=10) flow cytometry profiles of $MYB^{WT/WT}$ (black) and $MYB^{KD/KD}$ (red) K11bL cells (isotype control - solid grey).

Europe PMC Funders Author Manuscripts

Europe PMC Funders Author Manuscripts

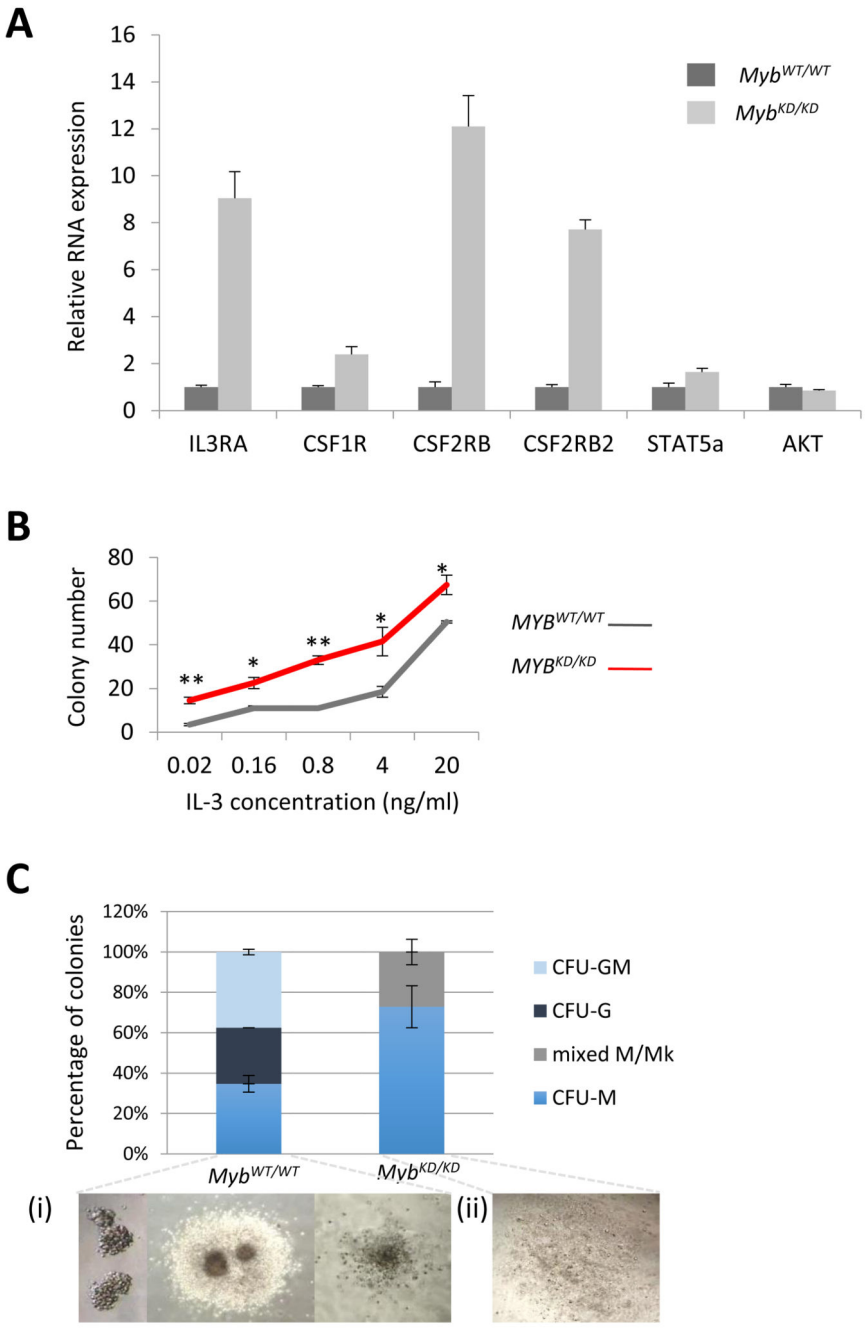

Figure 2.

A) Quantitative RT-PCR analysis of RNA expression for the indicated genes in K11bL cells (N=3). B) 500 sorted K11bL cells from $MYB^{WT/WT}$ and $MYB^{KD/KD}$ mice were plated in methylcellulose with varying concentrations of IL3. Colony number was scored after 7 days (N=2). C) Colony morphology of K11bL cells plated in M3234 containing 20ng/ml IL-3. Inset: i) Representative images of $MYB^{WT/WT}$ CFU-G (left), CFU-GM (middle), and CFU-M (right) colonies, and ii) $MYB^{KD/KD}$ CFU-M colonies

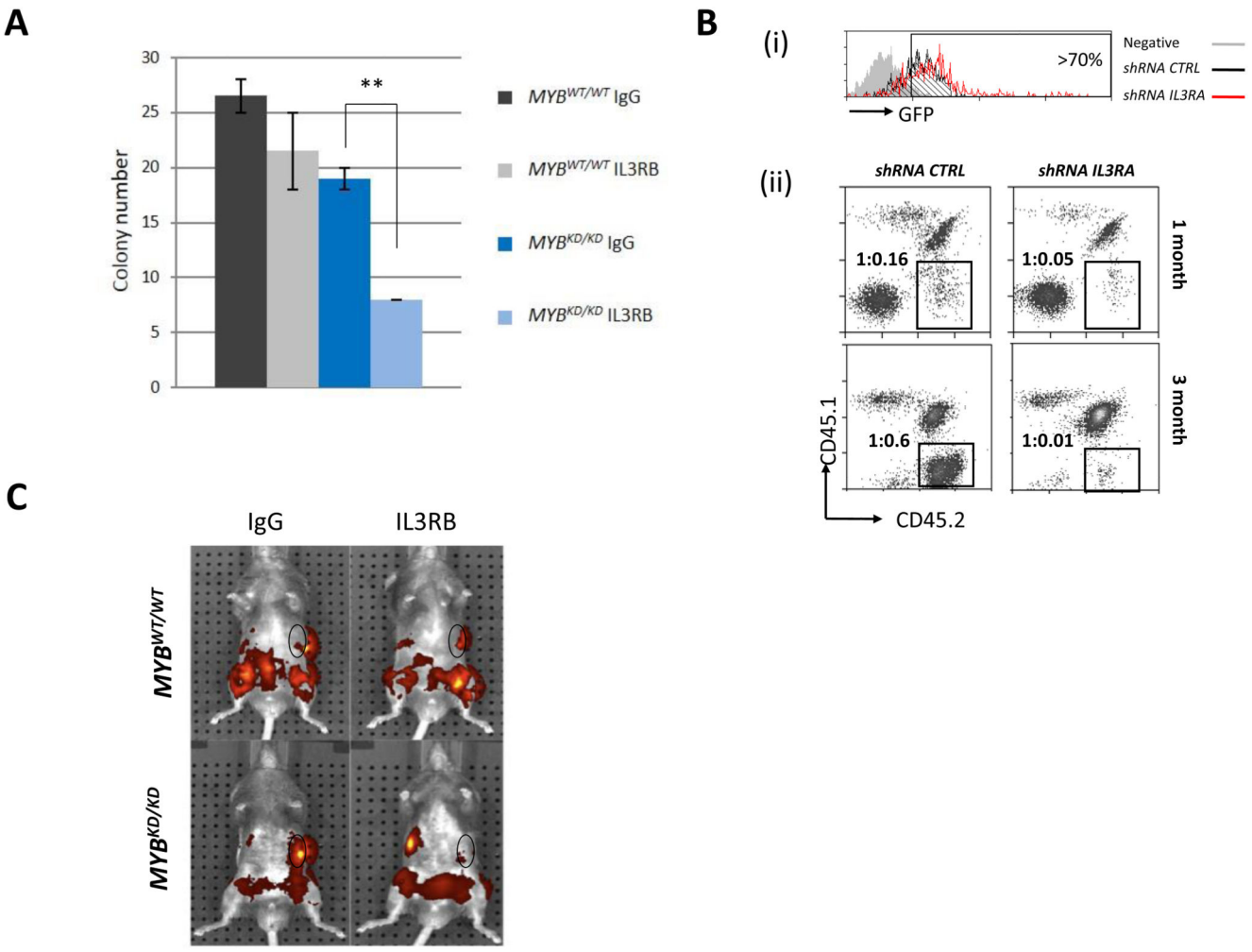

Figure 3.

A) Sorted K11bL cells were incubated in the presence of 30μg/ml of isotype or anti-IL3RB neutralizing antibody prior to plating in complete methylcellulose. Colony number was assayed after 7 days (**p≤0.01 N=3). B) *MYB*$^{KD/KD}$ K11bL cells were transduced with lentivirus carrying shRNA control or shRNA *Il3ra* before being injected into lethally irradiated mice: i) Transduced cells remaining in culture were assessed for transduction efficiency by GFP expression; ii) Peripheral blood from recipient mice was analyzed at 1 and 3 months post-transplantation to assess engraftment, the gates showing the CD45.2+ donor cells with the respective average reference:donor ratios. C) Staining with DiR and injection into lethally irradiated B6:SJL recipient mice. Recipients were imaged by IVIS after 24 hours by trans-illumination. The oval region highlighted indicates the region of the spleen measured. Images are representative of N=4.

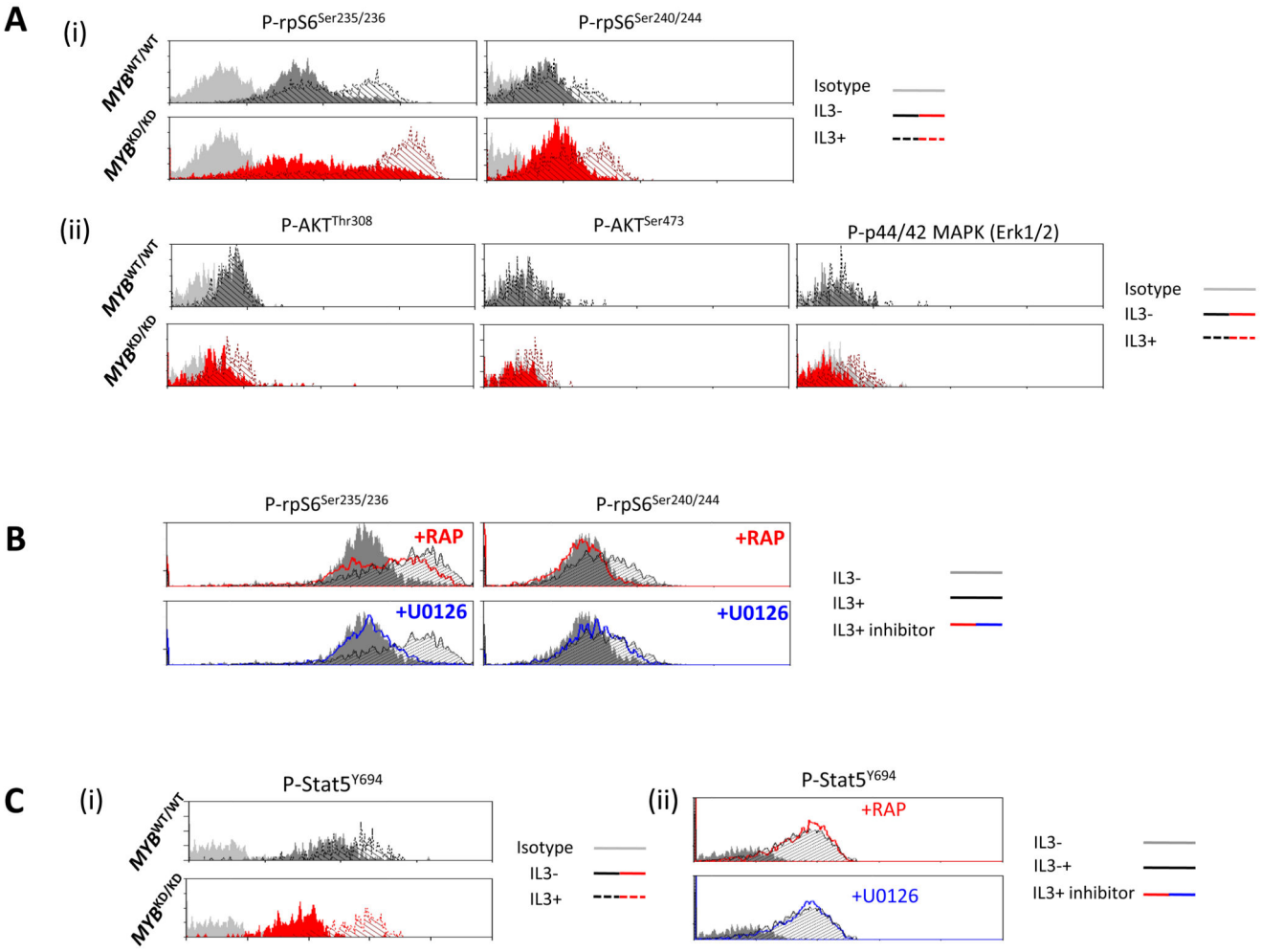

Figure 4.

Representative plots depicting phospho-flow analysis of K11bL cells, and the response to IL-3 stimulation. A) K11bL cells were serum-starved (solid black/red) prior to stimulation with 20ng/ml IL-3 (dashed black/red) for 15 min and then fixed and permeabilzed before staining with antibodies against i) phospho-rpS6$^{Ser235/236}$ and phosphor-rpS6$^{Ser240/244}$ (N=9). And ii) phospho-AKT^{Thr308}, phospho-AKT^{Ser473} and phospho-p44/42 MAPK following IL-3 stimulation (N=3). (isotype control – pale grey) B) *MYB*$^{KD/KD}$ K11bL cells were incubated with IL-3 in the presence and absence of mTOR inhibitor Rapamycin (1μM, red) or the MEK inhibitor U0126 (10μM, blue) (N=3). C) Staining of K11bL cells for P-Stat5^{Y694} following i) serum starvation (solid black/red) and stimulation with Il3 (dashed black/red) and ii) following stimulation with IL3 in the presence of either Rapamycin (red) or U0126 (blue).

Europe PMC Funders Author Manuscripts

Europe PMC Funders Author Manuscripts

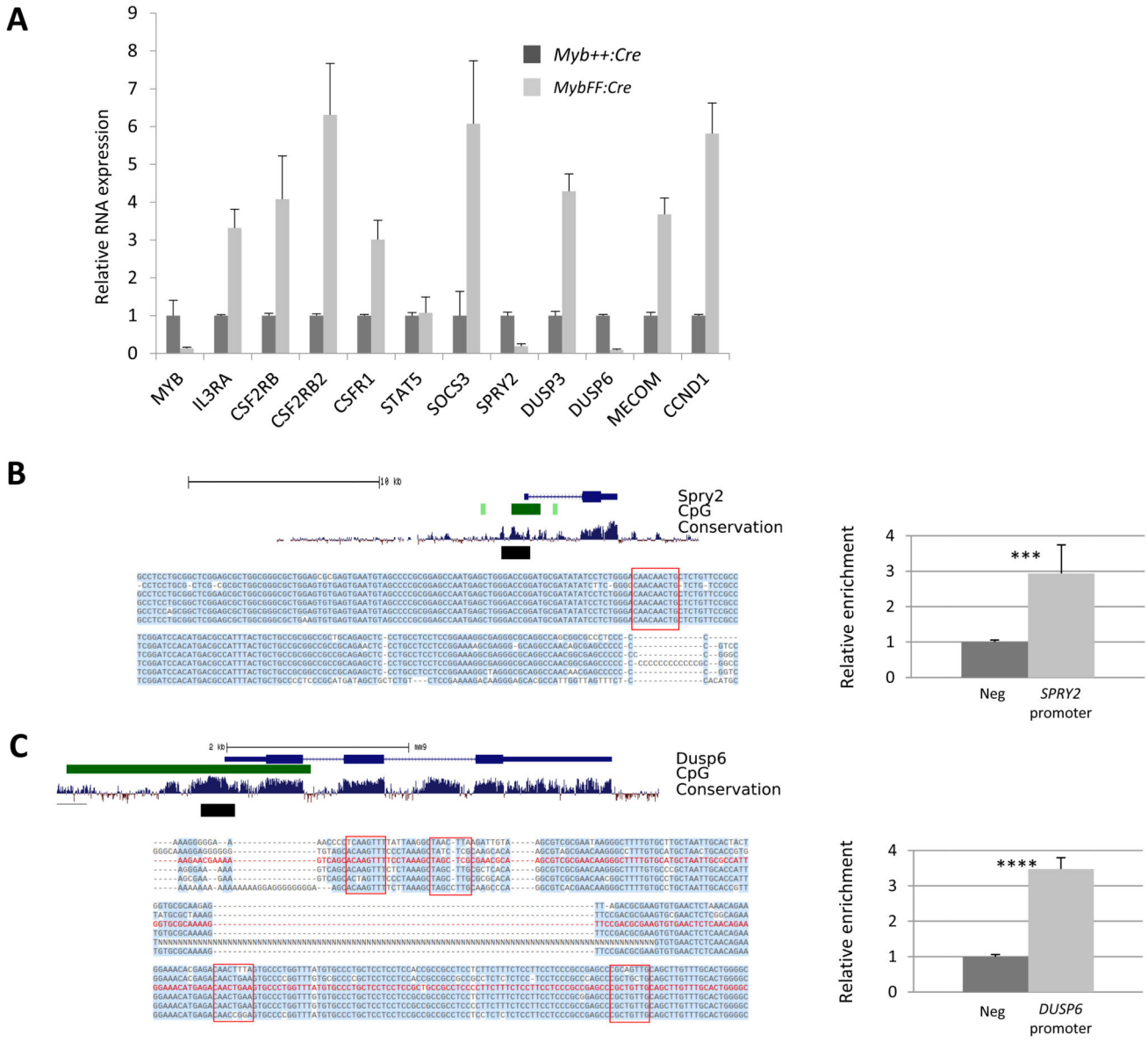

Figure 5.

A) K11bL cells from *MYB*$^{++}$*:Cre* and *MYB*^{FF}*:Cre* bone marrow were sorted 24 hours following intraperitoneal injection of pIpC to induce *Myb* gene deletion. Expression of the indicated signaling-associated genes was analyzed by quantitative RT-PCR and normalized against *β2M*. Error bars represent SEM (N=3). B) Alignment of mammalian sequences for the *SPRY2* gene, showing the gene exonic structures, the presence of CpG islands, the overall degree of sequence conservation, and the detail of the sequence conservation around potential MYB binding sites (red box) that were spanned by the Q-PCR primers. The histogram shows the results of quantitative PCR performed on HPC7 ChIP samples pulled down by MYB antibody and analysed for enrichment of binding on sequences for *SPRY2*. The histogram illustrates the relative enrichment as determined by Q-PCR (N=3, ***p≤0.001). C) A similar analysis to that described in (B) for the *DUSP6* gene.

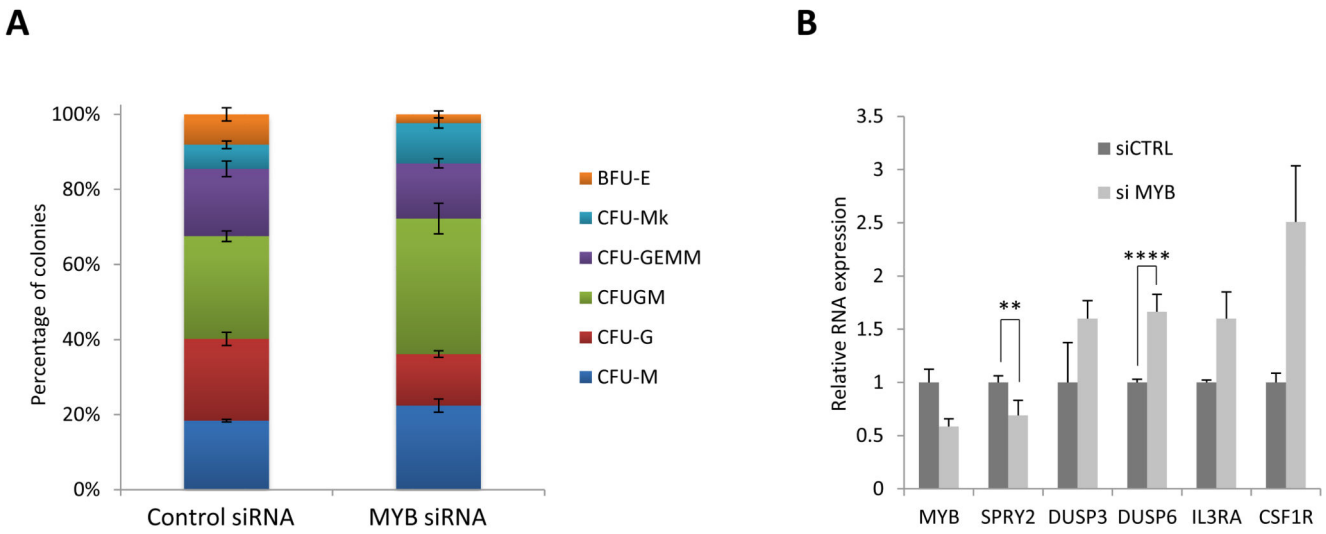

Figure 6.

A) Human CD34+ cells were isolated from human umbilical cord blood by FACS and transfected with either siRNA control or siRNA *MYB* and after 24 hours FAM+ cells were plated in complete methylcellulose and assayed for their ability to undergo full myeloid differentiation after 10 days in culture. B) Cells were also collected at 24 hours for the preparation and analysis of RNA expression. The histograms illustrate quantitative RT-PCR measurements of RNA expression for the *MYB, SPRY2, DUSP3, DUSP6, IL3RA* and *CSF1R* genes ** p≤0.001,**** p≤0.0001.

Europe PMC Funders Author Manuscripts

Europe PMC Funders Author Manuscripts

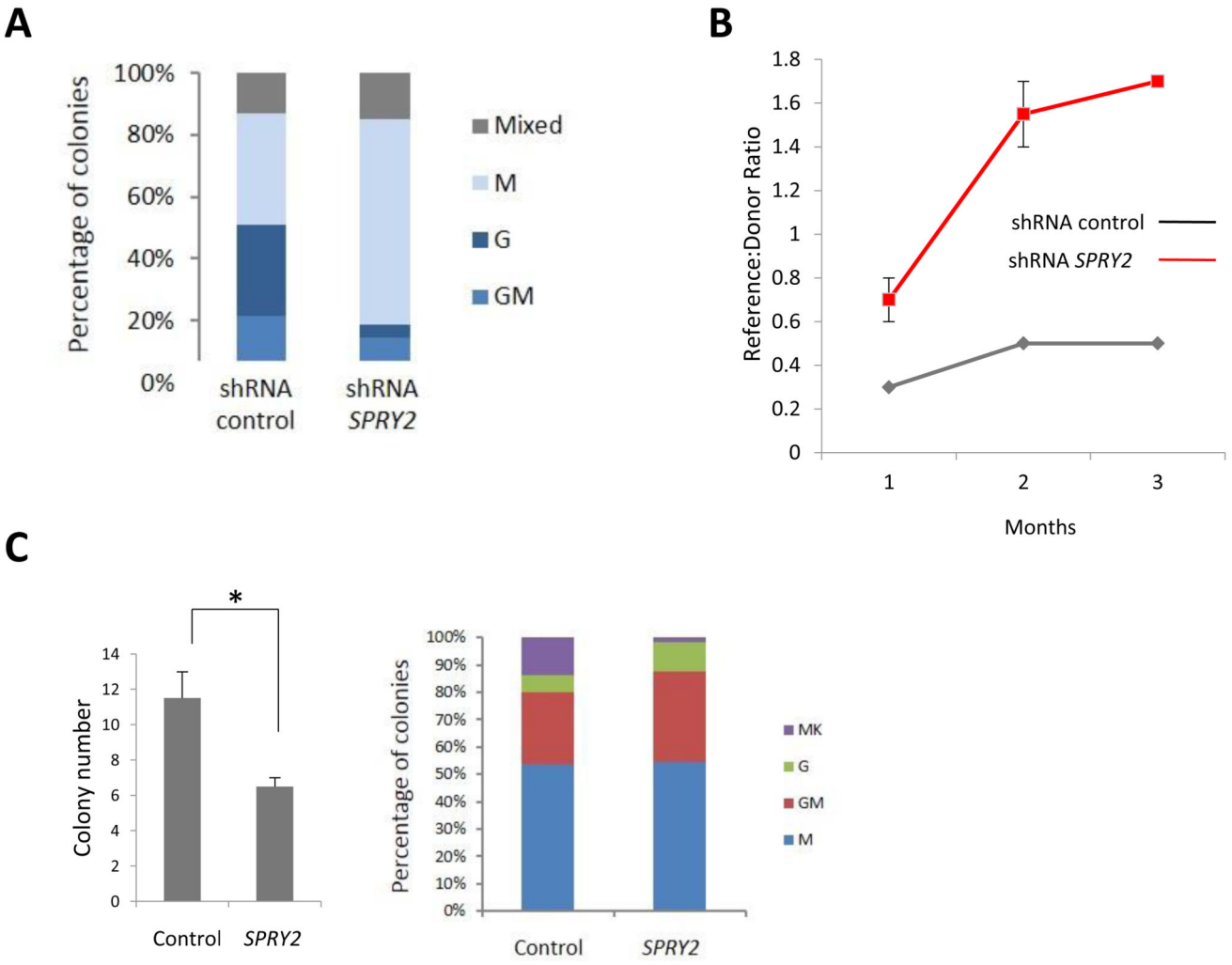

Figure 7.

A) *MYB*$^{WT/WT}$ K11bL cells were transduced with shRNA *SPRY2* and a corresponding shRNA control and 24 hours later were sorted on the basis of GFP expression and plated in complete methylcellulose. After 7 days in culture colonies were counted and their size scored GM: granulocyte / macrophage, G: Granulocyte, M: Macrophage, Mixed: containing all types. (N=3). B) *MYB*$^{WT/WT}$ K11bL cells were transduced with shRNA *SPRY2* and transplanted into lethally irradiated recipients. Peripheral blood was sampled monthly and the ratio of test donor to reference cells was determined. C) Overexpression of SPRY2 in *MYB*$^{KD/KD}$ K11bL cells followed by plating in complete methylcellulose (*p≤0.05) showing both colony number and myeloid differentiation potential in control and SPRY2 over expressing *MYB*$^{KD/KD}$ K11bL cells.

Europe PMC Funders Author Manuscripts

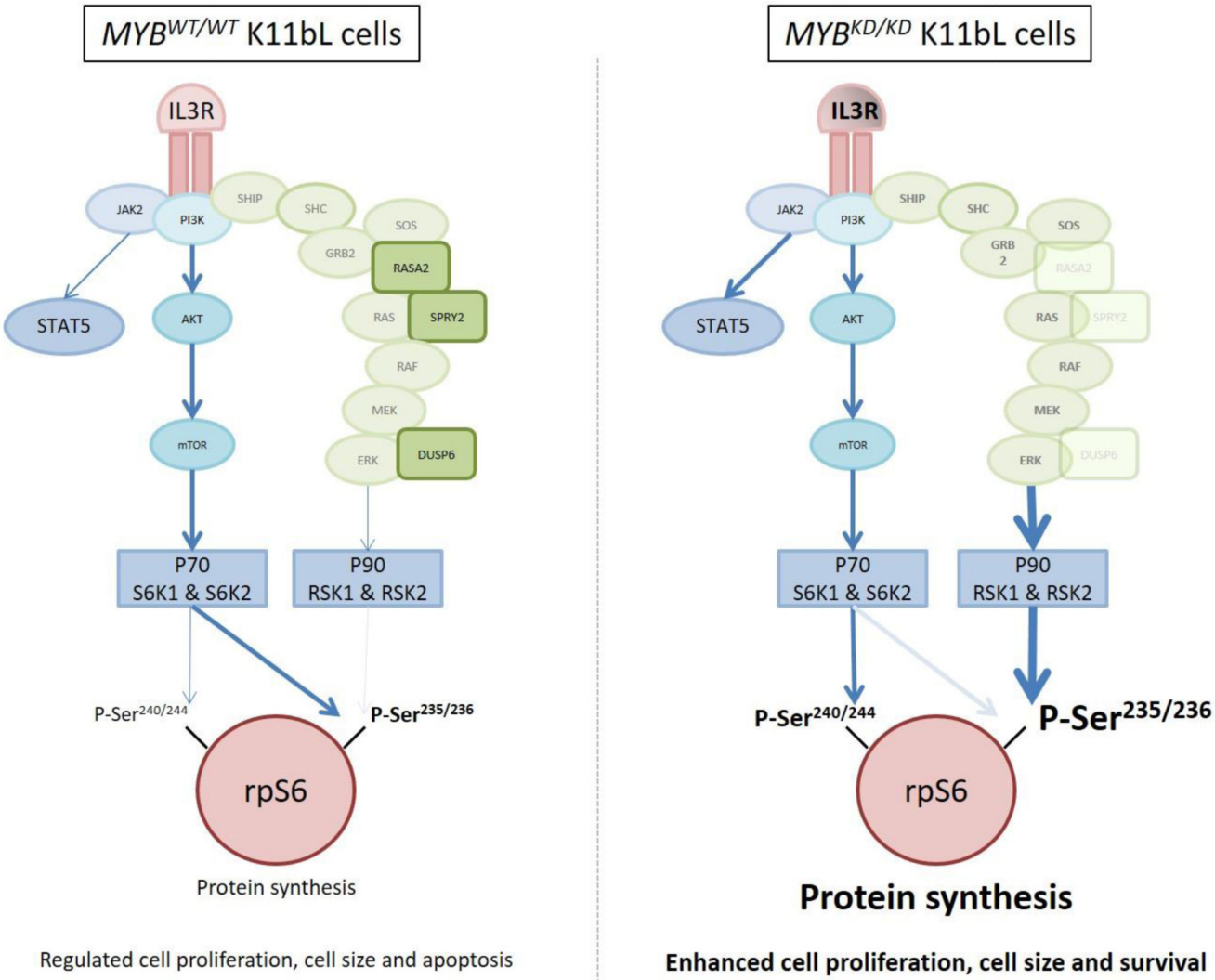

Figure 8. Working model of pathway utilization in *MYB*$^{WT/WT}$ and *MYB*$^{KD/KD}$ K11bL cells.

Schematic representation of IL-3 receptor signaling in K11bL cells, illustrating the differences in rpS6 phosphorylation observed in *MYB*$^{WT/WT}$ versus *MYB*$^{KD/KD}$ cells and how this appears to relate to changes in the signaling pathways utilized and the MYB-regulated signaling modulator SPRY2. The thickness of the arrows and the representation of the rpS6 phosphorylation sites gives a relative indication of the extent of pathway involvement and how this differs between the *MYB*$^{WT/WT}$ and *MYB*$^{KD/KD}$ cells.